The Prostate-Associated Lymphoid Tissue (PALT) Is Linked to the Expression of Homing Chemokines CXCL13 and CCL21

Emma Di Carlo,[1,2,3]* Salvatore Magnasco,[1,2,3] Tommaso D'Antuono,[1,2,3] Raffaele Tenaglia,[4] and Carlo Sorrentino[1,2,3]

[1]*Department of Oncology and Neurosciences, "G. d'Annunzio" University, Chieti, Italy*
[2]*CeSI Aging Research Center, "G. d'Annunzio" University Foundation, Chieti, Italy*
[3]*Department of Anatomic Pathology, "SS Annunziata" Hospital, Chieti, Italy*
[4]*Department of Urology, "SS Annunziata" Hospital, Chieti, Italy*

BACKGROUND. The genitourinary tract is regarded as part of the mucosal immune system. However, the structural and functional aspects of the human prostate-associated lymphoid tissue (PALT) have never been extensively explored.
METHODS. This article describes our investigation of this issue by means of immunohistological, confocal, and ultrastructural examination of the normal human prostate.
RESULTS. PALT consists of two main components: (1) intraepithelial leukocytes, namely $CD3^+$T cells with prevalent $CD8^+$ and $CD45RA^-CD45RO^+$ phenotype, sometimes $CD69^+$, followed by $CD94^+$NK, $CD11c^+$DCs, some expressing CD86, DC-$SIGN^+$DCs and a few B lymphocytes; (2) lymphoid aggregates, frequently below the epithelia, arranged in B cell follicles, endowed with a central $ICAM\text{-}1^+VCAM\text{-}1^+CD21^+$FDCs network expressing BLC/CXCL13, and parafollicular T cell areas crossed by $PNAd^+$HEV-like vessels showing SLC/CCL21 expression. Parafollicular areas were formed of prevalent $CD4^+$T lymphocytes, both $CD45RA^-$ and $CD45RO^+$, and intermingled with $CD11c^+$DCs. Germinal-center-containing follicles are few and their parafollicular areas are scantily infiltrated by $Foxp3^+CD69^-$ highly suppressive regulatory T cells. Most lymphoid follicles lack a distinct germinal center and their parafollicular area harbor numerous $Foxp3^+CD69^-$ cells.
CONCLUSIONS. Comparison with the tonsils shows that PALT displays immunomorphological features required for the onset of cellular and humoral immune responses, while its T regulatory cells appear to function as suppressor-regulators of T and B cell responses. *Prostate 67: 1070–1080, 2007.*

KEY WORDS: **human prostate; lymphoid follicles; chemokines; secondary lymphoid tissue; high endothelial venules**

INTRODUCTION

Mucosal-associated lymphoid tissues are immunologically active sites as the first line of defense against exogenous antigens [1]. Their distribution, in fact, reflects the risk of exposure to foreign materials or microorganisms: the oropharynx and nasopharynx contains Waldeyer's tonsillar ring; the bronchi, in some species, display follicle-associated epithelia (bronchus-associated lymphoid tissue, BALT) [2]; the digestive tract is endowed with scattered or grouped (Peyer's patches) lymphoid follicles (LFs) [3]. The genitourinary tract is also part of the mucosal immune system [4–6]. Its lymphoid tissue and ability to mount an immune

Grant sponsor: Fondazione Cassa di Risparmio della Provincia di Chieti (CariChieti), Italy.

*Correspondence to: Emma Di Carlo, ''G. d'Annunzio'' University, School of Medicine, Anatomic Pathology Section, ''SS Annunziata'' Hospital, Via dei Vestini, 66013 Chieti, Italy.
E-mail: edicarlo@unich.it
Received 5 February 2007; Accepted 20 March 2007
DOI 10.1002/pros.20604
Published online 1 May 2007 in Wiley InterScience (www.interscience.wiley.com).

response, however, have not been investigated in depth. The study described in this article, therefore, examines the architectural, immunological, and functional aspects of lymphoid tissue in the human prostate. This gland, in fact, comprises both lymphocyte aggregates embedded in its fibro-muscular meshwork, frequently below the epithelia, and a mixed population of intraepithelial leukocytes (IEL). Understanding of the immunological armamentarium of the prostate is needed to assess its ability to mount a local immune response against infections and tumors, and may be of assistance in predicting the efficacy of immunological anticancer strategies and the designing of vaccines against prostate cancer [7].

In this article, a description of the immunological and microarchitectural scenario of the prostate-associated lymphoid tissue (PALT) is followed by consideration of the question of its structural and functional similarity to the tonsil, namely a secondary lymphoid organ also endowed with an epithelial component and a paradigm of mucosal immunity.

MATERIALS AND METHODS

Patients, Histopathological and Ultrastructural Analyses

We examined a total of 137 prostates from patients who underwent prostatectomy for bladder cancer, and selected 35 normal prostates of untreated patients aged 62–70, which were histologically negative for prostate cancer or benign prostatic hyperplasia (BPH). Twenty-five of these 35 prostate specimens were embedded in paraffin and obtained from the archives of the Department of Anatomic Pathology. Ten prostates, collected during the last 5 years, were embedded in Killik frozen section medium (Bio-Optica, Milano, Italy), snap-frozen in liquid nitrogen and preserved at -80°C, after taking four or five 1 mm $\times$ 3 mm pieces that were fixed in cacodylate-buffered 2.5% glutaraldehyde. For histology, paraffin-embedded samples were sectioned at 4 μm and stained with hematoxylin-eosin. For electron microscopy, cacodylate-fixed samples were post-fixed in osmium tetroxide and embedded in Epon 812. Ultrathin sections were then stained with uranyl acetate-lead citrate.

Written informed consent was obtained from patients and the study was approved by the Ethical Committee of the ''SS. Annunziata'' Hospital. This investigation conformed with the principles outlined in the Declaration of Helsinki.

We also used formalin-fixed, paraffin-embedded, and frozen palatine tonsils excised in a non-inflamed state from patients who underwent tonsillectomy and were archived in the Anatomic Pathology Section of the ''SS. Annunziata'' Hospital of Chieti, Italy.

Antibodies and Immunohistochemistry

For immunohistochemistry on the formalin-fixed, paraffin-embedded samples, sections were treated with H_2O_2/3% for 5 min to inhibit endogenous peroxidase and then washed in H_2O. Antigen was unmasked by treatment with EDTA at pH 9 (prior to incubation with anti-CD8, anti-CD21, anti-CD68, anti-CD83, and anti-Von Willebrand factor [vWF] antibody [Ab]), or with citrate buffer at pH 6 (prior to incubation with anti-CD20, anti-CD138, and anti-peripheral lymph node addressin [PNAd] Abs) in a microwave oven (two 5 min courses).

The slices were then held for 20 min at room temperature. After washing in PBS/Tween-20, immunohistochemical staining was performed, as previously reported [8], with the primary Abs listed in Table I. To test prostate samples for IgA production, single immunofluorescent staining with FITC-conjugated Ab was performed on paraffin sections as previously reported [8].

For immunohistochemistry on the frozen samples, cryostat sections were fixed in acetone for 10 min. After washing in PBS/Tween-20, sections were stained, as reported [8], with the primary Abs listed in Table I.

PALT LFs were as counted as the number of $CD20^+$B cell follicles encircled by a $CD3^+$T cell ring (double immunostaining with anti-CD20/anti-CD3) in prostate sections obtained, from 25 formalin-fixed prostates, as follows. Each prostate was divided into five parts: the apex, the right-anterior quadrant, the right-posterior quadrant, the left-posterior quadrant, and the left-anterior quadrant. Each quadrant was sectioned at three equidistant levels. A slide (tissue section) was obtained from each level and one slide from the apex. Values are represented as the mean $\pm$ SD of LFs at 200$\times$ field evaluated by light microscopy on formalin-fixed, paraffin-embedded sections. Analyses of LFs and evaluation of the percentages of lymphocyte subsets (in LFs and inside the glandular epithelia) and of activated intraepithelial $CD11c^+$ and $CD3^+$ cells were performed (on double immunostained sections: anti-CD11c/anti-CD86, anti-CD3/anti-CD69, respectively) by two pathologists, E.D.C. and C.S, in a blind fashion. There was a substantial agreement (kappa value = 0.78) between their evaluations [9].

Double Immunohistochemical and Immunofluorescent Analyses

Double immunohistochemistry on paraffin-embedded tissue sections was performed with anti-CD20, anti-CD21, anti-CD8, anti-CD4, anti-CD3, anti-forkhead box P3 (Foxp3), anti-CD45RA, anti-CD45RO, anti-CD57, and anti-CD69 Abs by using the EnVision™ G/2 Doublestain System, Rabbit/Mouse (Dako, Glostrup,

TABLE I. Antibodies Used in Immunostaining

Antibody	Clone	Origin	Source
Paraffin sections			
PNAd[a]	MECA-79	Rat	BD (Franklin Lakes, NJ)
Bcl-6	PG-B6p	Mouse	Dako
CD3[a]	F7.2.38	Mouse	Dako
CD4	MT310	Mouse	Dako
CD8	C8/144B	Mouse	Dako
CD20[a]	L26	Mouse	Dako
CD21[a]	1F8	Mouse	Dako
CD45RA	4KB5	Mouse	Dako
CD45RO	UCHL1	Mouse	Dako
CD68	PG-M1	Mouse	Dako
CD79a	JCB117	Mouse	Dako
CD138	MI15	Mouse	Dako
IgA		Rabbit	Dako
Ki-67	MIB-1	Mouse	Dako
vWF	F8/86	Mouse	Dako
DC-LAMP	104.G4	Mouse	Beckman Coulter (Fullerton, CA)
CD69	CH11	Mouse	Lab Vision (Fremont, CA)
CD83	1H4b	Mouse	Vision BioSystems (Newcastle Upon Tyne, UK)
Foxp3	mAbcam 22510	Mouse	Abcam (Cambridge, UK)
Frozen sections			
DC-SIGN	DCN46	Mouse	BD
CD94	HP-3D9	Mouse	BD
TCR$\gamma\delta$	B1	Mouse	BD
CD11c	KB90	Mouse	Dako
CD86	BU63	Mouse	Dako
CCL21		Goat	R&D (Minneapolis, MN)
CXCL13	53610.11	Mouse	R&D
CXCR5	51505.111	Mouse	R&D
CCR7		Goat	Santa Cruz (Santa Cruz, CA)
CD69	MLR-3	Mouse	Dr. S. Ferrini, Genova, Italy

[a]Abs used on both paraffin and cryostat sections.

Denmark) according to the manufacturer's protocol and analyzed under a Leica DMLB light microscope (Leica, Wetzlar, Germany).

Double immunofluorescent staining on acetone-fixed frozen sections was performed with anti-CD3, anti-CD20, anti-CD21, anti-CD11c, anti-CD86, anti-PNAd, anti-DC-SIGN, and anti-CCL21 Abs, as previously reported [8], and analyzed under a Zeiss LSM 510 Meta confocal microscope (Zeiss, Oberkochen, Germany).

RESULTS

Structure and Immunophenotype of the PALT

PALT consists of two components: (1) a diffuse collection of isolated lymphoid aggregates lying in the fibromuscular stroma of the prostate and frequently close to the double-layered glandular epithelium of the acini and ducts, above the basement membrane and, (2) a population of IEL infiltrating the epithelia and endowed with a distinctive phenotype.

Lymphoid aggregates occasionally consisted of an unorganized infiltrate of $CD20^+$B and $CD3^+$T lymphocytes (Fig. 1, panel A, a) (both $CD8^+$T and $CD4^+$T including a small fraction of $Foxp3^+$Treg cells) with intermingled dendritic cell (DC)-specific, ICAM-3 grabbing, non-integrin $(DC\text{-}SIGN)^+$DCs (Fig. 1, panel A, b). Most aggregates (a mean of 5.3 ± 2.4 per quadrant, including the apex), were scattered in the whole of the prostatic stroma and were arranged in well-defined $CD20^+$B-lymphocyte follicles (B cells constituting about 50% of the whole aggregate) centered around networks of $CD21^+$follicular dendritic cells (FDCs) (Fig. 1, panel A, c), usually expressing intercellular adhesion molecule 1 (ICAM-1) and vascular cell adhesion molecule 1 (VCAM-1), and surrounded by parafollicular $CD3^+$T lymphocyte areas (Fig. 1, panel A, d). These were formed by naïve

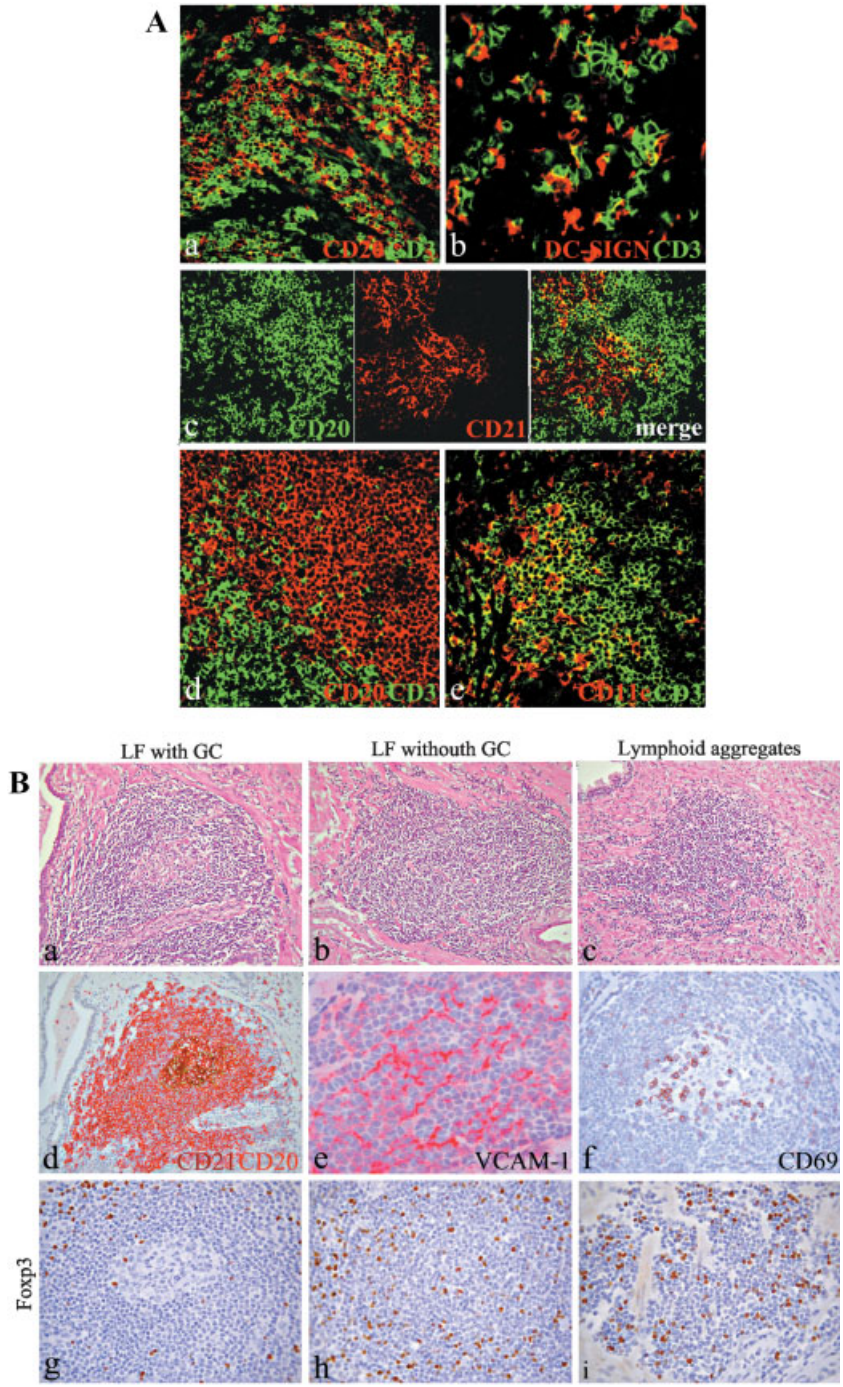

Fig. 1. **Panel A**: Laser scanning confocal images of organized (LF) and unorganized lymphoid aggregates in PALT. Immunophenotyping of an unorganized lymphoid infiltrate homing to the prostatic stroma reveals a mixed population of $CD20^+$B and $CD3^+$T lymphocytes (**a**) tightly interacting with DC-$SIGN^+$DCs (**b**). Most aggregates, however, are organized in $CD20^+$B-lymphocyte follicles centered around a network of $CD21^+$FDCs (**c**) and surrounded by parafollicular $CD3^+$T cell areas (**d**) usually infiltrated by $CD11c^+$DCs (**e**). (a,c–e: 400×; b: 630×.) **Panel B**: Histological and immunohistochemical features of primary and secondary LFs and unorganized lymphoid aggregates in PALT. Organized lymphoid aggregates may show the feature of a secondary LF containing the typical GC with centroblasts and centrocytes (a) and formed of a pool of $CD20^+$B lymphocytes with intermingled $CD21^+$FDCs (d) expressing VCAM-1 (e). GCs are characterized by $CD69^+$ Th cells (**f**), while the T cell area and T-B cell border zone are barely infiltrated by $Foxp3^+$Treg cells (**g**), mostly $CD69^-$ (f). More frequently LFs are devoid of GC (primary LF) and are formed by small lymphocytes (b). They are usually infiltrated by numerous $Foxp3^+$Treg cells (**h**) similarly to what is observed in unorganized lymphoid aggregates (c,**i**). LF, lymphoid follicle; GC, germinal center. (a–d: 200×; f–i: 400×; e: 630×.)

$CD45RA^+$ and memory $CD45RO^+$ lymphocytes (data not shown) with CD4 (~25% of the aggregate) and CD8 (~15% of the aggregate) phenotype intermingled with myeloid $CD11c^+$DCs (~10% of the aggregate) (Fig. 1, panel A, e).

A germinal center (GC), containing ICAM-1^+VCAM-$1^+$$CD21^+$FDCs and showing centroblasts, centrocytes, and $CD69^+$ cells (Fig. 1, panel B, a,d,e,f) which co-localized with $CD57^+$T helper (Th) cells (not shown) [10], was detectable in some organized LFs (6 out of 25 prostates, i.e., ~25%. Two prostates harbored two and the other four only one GC-containing follicle). The T cell zone up to the border with the B cell area contained a scanty population of $Foxp3^+$regulatory T (Treg) lymphocytes lacking CD69 expression (Fig. 1, panel B, g,f), some of which had infiltrated the GC. The T cell zone also harbored numerous $CD68^+$ macrophages, $CD86^+CD11c^+$DCs, some dendritic cell-lysosomal associated membrane protein (DC-LAMP)$^+$ and $CD83^+$ DCs. A few $CD138^+$ plasma cells were located at the LF periphery.

Most LFs lacked distinct GC (Fig. 1, panel B, b) and $CD57^+$ Th cells and usually contained numerous DC-$SIGN^+$DCs and $Foxp3^+$Treg lymphocytes (Fig. 1, panel B, h) negative for CD69 (not shown) as also observed in the unorganized aggregates (Fig. 1, panel B, c,i).

IEL were basically composed of $CD3^+$TCRαβ, with rare TCRγδ, both $CD8^+$, which prevailed (about 70% of $CD3^+$T cells), and $CD4^+$ diffusely penetrating the epithelium (Fig. 2a and inset). They also crowded the stroma just below the basal membrane, particularly when they expanded from the edge of periglandular LFs. Lymphocytes, frequently $CD45RO^+$, may express the CD69 early activation marker (from 10% to 30% of the $CD3^+$ cells) (Fig. 2b). The epithelium was also penetrated by a discrete number of $CD94^+$NK cells (Fig. 2c) followed by $CD11c^+$DCs which may express the CD86 co-stimulatory molecule (from 10% to 50% of the $CD11c^+$ cells) (Fig. 2d,e). DC-$SIGN^+$DCs (Fig. 2f) and $CD68^+$ macrophages (Fig. 2g) were less represented. They were mostly scattered in the stroma and frequently crowded below the basal membrane. DC-$LAMP^+$ and $CD83^+$ DCs were almost absent in the epithelium and stroma. Lastly, $CD20^+$ or $CD79a^+$ B cells were also more frequently crowded below the basal membrane than present among the epithelial cells (Fig. 2h), like the $CD138^+$ plasma cells releasing IgA in the epithelia (Fig. 2i).

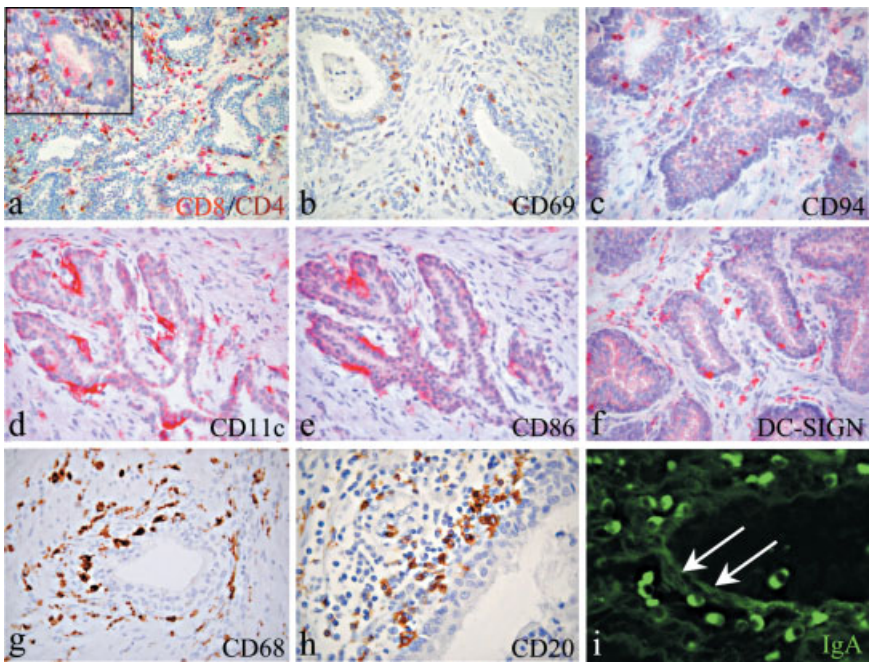

Fig. 2. Immunohistochemical characterization of leukocyte populations infiltrating the prostatic glandular epithelium. Double immunohistochemistry shows that prostatic epithelia are usually fairly infiltrated by lymphocytes, mostly $CD8^+$ (red) rather than $CD4^+$ (brown) (**a** and inset). They may express the CD69 early activation marker (**b**). The epithelium was also penetrated by a discrete number of $CD94^+$NK cells (**c**) followed by CDIIc$^+$DCs (**d**) which may express the CD86 co-stimulatory molecule (**e**). DC-$SIGN^+$DCs (**f**) and CD68 macrophages (**g**) barely infiltrate the epithelium and especially the stroma. $CD20^+$B lymphocytes may sometimes be found underneath the basal membrane and rarely within epithelial cells (**h**) as also plasma cells producing IgA evidenced by single immunofluorescence analyses (**i**) (white arrows indicate the basal membrane). (a: 200×; b–g: 400×; h,i: 630×.)

Expression of Homing Chemokine-Receptor Systems in the PALT

Since the architectural and immunological features of the prostate LFs were very similar to those of LFs in secondary lymphoid organs, we set out to determine whether they were also associated with the expression of lymphocyte homing molecules playing key roles in lymphoid neogenesis and homeostasis [11–14].

The B-lymphocyte chemoattractant (BLC) also called BCA-1 (B-cell-attracting chemokine-1) or CXCL13, could be expressed inside LFs, with or without GC, probably by FDCs (as revealed by the reticular-shaped immunostaining in the follicle center) (Fig. 3a) typically endowed with branched cytoplasmic processes. In some of the less organized aggregates, it was more frequently expressed by fibroblast-like mesenchymal cells (Fig. 3b) that were also tightly intermingled (like the FDCs) within B lymphocytes. The BLC receptor, CXCR5 (Burkitt lymphoma receptor-1, BLR1), was usually detected on the surface of round cells, mostly B lymphocytes, resident in the innermost area of LFs (Fig. 3c).

LFs were supplied by a poorly developed microvascular network, of which some lengths displayed a constant expression of PNAd (Fig. 3d) and typical feature of high endothelial venules (HEV) appearing as plumped vessels formed of cubical endothelial cells, located in the parafollicular T cell area, frequently at the edge of the B cell follicle (Fig. 3e).

Production of the potent T cell attractant secondary lymphoid-tissue chemokine (SLC) also known as TCA-4, Exodus-2, 6Ckine or CCL21, was evidenced in endothelial cells forming HEV-like vessels (Fig. 3f). The CCL21 receptor, namely CCR7, was expressed by lymphocytes (small round cells), but particularly by cells with DC morphology (endowed with elongated or ramified cytoplasm processes) homing to the parafollicular T cell areas (Fig. 3g).

Comparisons Between PALT and Tonsil Microarchitecture

PALT includes immune cell aggregates mostly homing close to the glandular epithelium and mimicking a few structural and functional aspects typical of secondary lymphoid tissues. We therefore set out to determine whether its immunological and microarchitectural features are comparable with those of the tonsil, in other words a lymphoepithelial organ representative of mucosa-associated lymphoid tissue (MALT). (Findings are summarized in Table II.)

PALT and tonsil are mostly composed of round, primary LFs (usually smaller in PALT) and secondary GC-containing LFs which develop after antigenic stimulation [15]. They are more frequent in the tonsil and very occasional in the prostate.

GCs are typically surrounded by a mantle of small B cells (the mantle zone) and formed by follicular center B cells (centroblasts and centrocytes) (Fig. 4, panel A, a,b), macrophages and $CD21^{+}$FDCs (Fig. 4, panel A, c,d). The expression of B-cell lymphoma 6 protein (bcl-6), the proto-oncogene encoding for a POZ/zinc finger

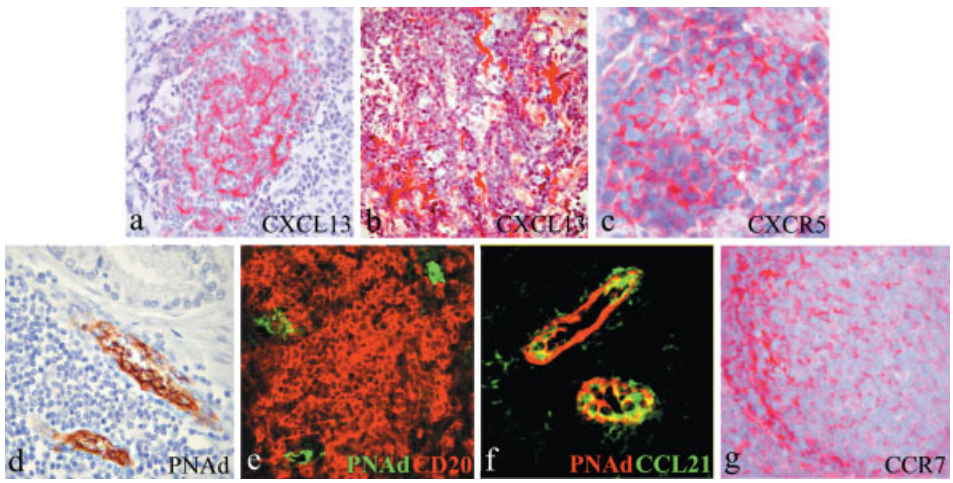

Fig. 3. Immunohistochemical evidences of lymphocyte homing chemokine-receptor system and PNAd expression in PALT LFs. The inner zone of LF shows a distinct CXCLI3 expression closely following the typical shape and distribution of FDCs (**a**) and of fibroblast-like cells in less organized lymphoid aggregates (**b**). The expression of the CXCR5 receptor is localized on the surface of round cells, most probably B lymphocytes, also homing the inner LF (**c**). Small vessels formed by high endothelial cells and passing through the T cell area (**d**), frequently at the edge of the B cell follicle (as assessed by double immunofluorescence and confocal analyses) expressed PNAd (**e**). These vessels appear to express CCL2I (as assessed by double immunofluorescence and confocal analyses) (**f**). Expression of the CCR7 receptor is localized on small round cells, probably lymphocytes, and particularly on DC-like cells homing to the parafollicular T cell areas of LFs (**g**). (a,b,e,f,g: 400×; c,d: 630×.)

TABLE II. Comparison of the Main Structural and Functional Features of PALT and Tonsil

Immunomorphological features[a]	PALT	Tonsil
LFs with organized B and T cell areas	+	++
$CD20^+$B-lymphocyte follicle centered around FDC network	+	++
GCs development	±	++
Ki-67^+ and bcl-6^+ GC cells	+	+
Follicular CXCL13-CXCR5 expression	+	++
Microvascularization of LFs	±	±
HEV-PNAd expression	++	++
HEV-CCL21 expression	+	++
Presence of IEL	++	++

[a]The presence of immunomorphological features was scored as absent (−), low (±), moderate (+), or frequent (++).

transcriptional repressor and necessary for GC formation [16,17], highlighted the nuclei of centroblasts, centrocytes and possibly occasional T cells (Fig. 4, panel A, e,f).

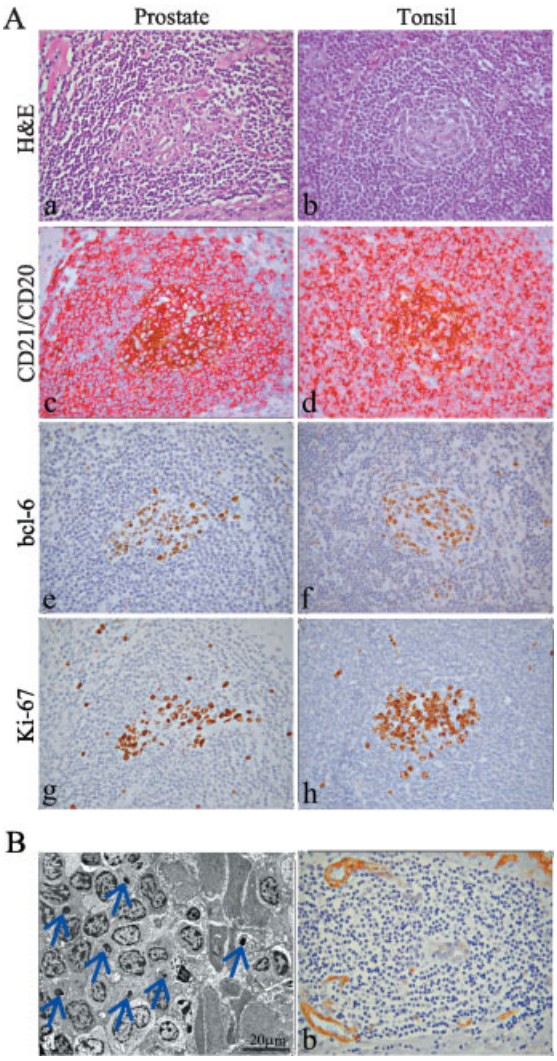

GC proliferation is indicative of ongoing humoral Ab production [18]. It was revealed by Ki-67 positivity of GC B cells in both PALT and tonsil (Fig. 4, panel A, g,h). Ultrastructural features of apoptosis (chromatin hypercondensation and apoptotic bodies) were observed in PALT LFs (Fig. 4, panel B, a) and tonsil LFs (not shown).

The FDC-B cell-rich compartment of PALT LFs expressed, albeit inconstantly or sometimes barely detectably, the chemokine-receptor system CXCL13-CXCR5 regularly observed in the B cell-rich follicular compartment of the tonsil [19].

As assessed by vWF immunostaining, the tonsil and PALT LFs lacked a well-developed microvascular network (Fig. 4, panel B, b). Expression of CCL21 in $PNAd^+$HEV vessels was usual in the tonsil, but less frequent in PALT LFs.

Both the stratified squamous epithelium covering the tonsil's lymphoid tissue and the double-layered epithelium of prostatic acini and ducts house moderate leukocyte infiltrates, though their component populations were dissimilar. By contrast with the prostatic epithelium, in the tonsilar epithelium $CD3^+$ T cells

Fig. 4. **Panel A**: Comparisons of the histological and immunohistochemical features of PALT and tonsil secondary LFs. GCs in PALT LFs (**a**) are similar to those in tonsil LFs (**b**) and typically formed by centroblasts and centrocytes. Both are centered by a network of $CD21^+$FDCs as shown by double immunohistochemistry (**c**,**d**; CD21 brown, CD20 red) and typically show the expression of bcl-6 (**e**,**f**), fundamental for GC development and functionality, and Ki-67 (**g**,**h**) indicating GC cell proliferation. (a–h: 400×) **Panel B**: Evidences of apoptotic features and defective microvascular network in PALT LFs. Apoptotic events take place in GCs developing in PALT LFs, as shown by ultrastructural images of chromatin hypercondensation and the appearance of apoptotic bodies (blue arrows in a). PALT LFs show a poorly developed microvascular network, as assessed by vWF immunostaining (b). (b: 400×.)

(rarely TCRγδ) were mainly $CD4^+$ as opposed to $CD8^+$ cells. The tonsilar epithelium was fairly infiltrated, especially its basal layers, by immature $CD1a^+$ and DC-$SIGN^+$ DCs, whereas DC-$LAMP^+$ and $CD83^+$ DCs were almost completely absent. $CD20^+$B were almost absent, $CD79a^+$B lymphocytes and $CD94^+$NK cells were few.

DISCUSSION

Interest in the mucosal immunity has been chiefly renewed for three reasons: (a) peripheral lymphoid organs are not absolutely required for the initiation of immune responses that could take place in the mucosa [20,21], (b) the emerging concept of a common mucosal recirculation system [22] by which immune cells activated (e.g., by vaccination) at certain mucosal sites are able to migrate to distant mucosal surfaces [23–25], (c) the possibility of developing new anti-cancer vaccines by exploiting the mucosal immune system potential [26]. Prostate cancer is the most common non-cutaneous tumor in humans [27] and the human prostate is endowed with a lympho-epithelial component which is part of the genito-urinary mucosal immunity. Thus, understanding of its structural and functional features has become a pressing need. Till now, only a few studies have been focused on immune cell populations and mediators characterizing the normal human prostate tissue [28,29]. Our immunomorphological investigation of the prostate lymphoid tissue equipment namely PALT, aims to shed light on this issue. The main points emerging from our data may be summarized as follow:

(a) The human prostate harbors a variety of immune cell populations at various activation and differentiation stages that either infiltrate the glandular epithelia, or are scattered or aggregated in the stroma. Therefore, immune effector elements are directly integrated in both the stromal and the epithelial compartments and establish an intimate relationship with them.
(b) In the stroma, often close to the epithelium, lymphocyte aggregates may be arranged in distinct B cell follicles, sometimes developing GCs, and parafollicular T cell areas giving rise to LFs. These LFs share structural and functional features with LFs in lymphoid organs (Ki-67 and bcl-6 positivity together with apoptotic features characterize GC cells of both PALT and tonsil). Therefore, it may be inferred that the prostate, like secondary lymphoid organs, can mount B and T adaptive immune responses.
(c) $Foxp3^+$Treg cells are scattered in the prostatic stroma intermingled with other leukocyte subsets. They infiltrate lymphoid aggregates and may also be found in primary or secondary LFs. Therefore, in the prostate, as in secondary lymphoid organs, Treg cells could inhibit T cell activation and T cell-mediated immune responses [30,31], but also B cell Ig production [32,33].

The genitourinary tract functions in close proximity to the outside environment, yet must remain free of microbial colonization to avoid disease [34]. The urethra appears to be the sole site of antigen entry in the prostate, but curiously, all the prostate tubulo-alveolar glands are more or less housed by leukocytes which may be, at least in part, functionally activated as revealed by co-stimulatory molecule, CD86, and activation antigen, CD69, expression by intra-epithelial $CD11c^+$DCs and $CD3^+$T lymphocytes, respectively.

The variable $CD11c^+CD86^+/CD11c^+CD86^-$ ratio depicts the balance between immunogenic and tolerogenic intra-epithelial DCs [35], while the activated ($CD69^+$) memory ($CD45RO^+$) phenotype of intraepithelial lymphocytes may result from intra-epithelial accumulation of lymphocytes previously primed in conventional lymphoid organ or, in accordance with the concept of ''a common mucosal recirculation system,'' by their migration from other mucosal sites were they have experienced antigen and been activated.

The steady ''permeation'' of glandular epithelia by T lymphocytes, DCs, macrophages, and NK cells strongly suggests the possibility that selective epithelial-derived mediators account for the epithelial tropism of these immune cells and probably affect their functional state [36,37].

In addition to glandular epithelia, the stromal component of the prostate does not appear to shirk the building of PALT. Together with FDCs in LFs, in fact, mesenchymal elements, in the form of fibroblast-like cells, in less organized lymphoid aggregates both express ICAM-1 and VCAM-1 as FDCs and cooperate in the production of CXCL13 which control B cell migration and thus the organization of B cell follicles [38,39]. Involvement of mesenchymal cells in lymphoid tissue organogenesis has been demonstrated [40,41]. The question of whether, in the prostate microenvironment, these cells also express lymphotoxin β receptor (LTβR) or TNF receptors (TNFRs) and may respond to lymphotoxin, which may trigger adhesion molecule and CXCL13 expression [42,41], remains to be investigated.

The prostatic stroma also harbors two key elements of the PALT structure, namely FDCs and HEV-like vessels. The former, usually arranged in a center-follicular network, are probably needed to support GC

germinal center reactions and regulate B cell response in the prostate as in lymphoid organs [43], while the latter, morphologically (cuboidal feature) and functionally (PNAd and CCL21 expression) mimicking lymphoid tissue HEV, may be crucial for naïve lymphocyte recruitment and enter [44–46] the T cell zone of prostate LFs. Our confocal analyses localize CCL21 near PNAd expression, but do not provide any definite information about its direct production by HEV-like vessels. Thus the possibility that, as in the human tonsil, the expression of CCL21 by prostate HEV-like vessels is consequent to transcytosis of the chemokine [47] cannot be ruled out.

The presence of CXCL13-CXCR5 and CCL21-CCR7 homing chemokine-receptor systems together with $PNAd^+$HEV-like vessels respectively in the B and T cell zones of prostate LFs is consistent with the classical lymphoid architecture [10,11] also detectable at mucosal sites [1] where they provide signals for lymphocyte migration and the building of organized lymphoid structures. The great variability in the number and stage of development of LFs contained in such structures (tonsil, BALT or others) closely depends on the frequency and type of antigenic stimuli they receive. The relatively few LFs usually detectable in the normal prostate may thus be presumed to undergo quantitative and morphological changes when inflammatory or malignant lesions occur. The main aim of this study was to depict the immunological features of the normal adult prostate, whereas the question whether these features may change during prostatitis, BPH or carcinoma was not addressed.

Importantly, within both organized and unorganized lymphoid structures and within leukocytes scattered in the stroma, we found $Foxp3^+$Treg cells. Recently, it has been shown that benign prostate tissue is barely infiltrated by $CD4^+CD25^+Foxp3^+$ lymphocytes [48]. We here report that the highly suppressive $Foxp3^+CD69^-$Treg cell subset [33] penetrates lymphoid aggregates. It is well represented in those not organized or those lacking a distinct GC and less numerous in GC-containing follicles typically endowed with $CD57^+CD69^+$ Th cells and where the B cell response is going on. As recently observed in the tonsil [33], in these reactive follicles $Foxp3^+$Treg cells are located in the T cell zone up to the border with the B cell area and some of them infiltrate the latter as far as the GC. This feature strongly suggests that, as in lymphoid tissues, in the PALT Treg cells suppress GC-Th cells and the B cell Ig response.

In conclusion, this study provides the first demonstration that the human prostate is endowed with a lymphoid component, namely PALT, whose structural and functional features may enable the gland to mount and/or expand other site-triggered immune responses. An intriguing question is whether PALT is inducible by external factors such as high antigen load, infection and inflammation, as in the case of BALT (which occurs in only 40% of healthy adolescents and children) [49] or, alternatively, its development is genetically predetermined as observed for other compartments of the human mucosal immune system (which appear before birth at predictable sites) [50]. This is an important research area since definition of the immunological tools in the human prostate is an essential step towards the elaboration of vaccines and forms of immunotherapy to prevent and treat prostate cancer.

ACKNOWLEDGMENTS

A special word of thanks to Prof. John Iliffe for editing the manuscript.

REFERENCES

1. Brandtzaeg P, Pabst R. Let's go mucosal: Communication on slippery ground. Trends Immunol 2004;25:570–577.
2. Bienenstock J, McDermott MR. Bronchus- and nasal-associated lymphoid tissues. Immunol Rev 2005;206:22–31.
3. Lanning DK, Rhee KJ, Knight KL. Intestinal bacteria and development of the B-lymphocyte repertoire. Trends Immunol 2005;26:419–425.
4. Fritz FJ, Westermann J, Pabst R. The mucosa of the male genital tract; part of the common mucosal secretory immune system? Eur J Immunol 1989;19:475–479.
5. Johansson M, Lycke NY. Immunology of the human genital tract. Curr Opin Infect Dis 2003;16:43–49.
6. Lamm ME, Mestecky J. Immunology and immunopathology of the genitourinary tract and mammary gland: An overview. In: Mestecky J, Bienenstock J, Lamm ME, Mayer L, McGhee JR, Strober W, editors. Mucosal immunology. 3rd edition. Amsterdam: Elsevier/Academic Press; 2005. pp 1575–1578.
7. Marrari A, Iero M, Pilla L, Villa S, Salvioni R, Valdagni R, Parmiani G, Rivoltini L. Vaccination therapy in prostate cancer. Cancer Immunol Immunother 2007;56:429–445.
8. Di Carlo E, Cappello P, Sorrentino C, D'Antuono T, Pellicciotta A, Giovarelli MG, Forni G, Musiani P, Triebel F. Immunological mechanisms elicited at the tumour site by lymphocyte activation gene-3 (LAG-3) versus IL-12: Sharing a common Th1 anti-tumour immune pathway. J Pathol 2005;205:82–91.
9. Landis JR, Koch GG. The measurement of observer agreement for categorical data. Biometrics 1977;33:159–174.
10. Kim JR, Lim HW, Kang SG, Hillsamer P, Kim CH. Human CD57+ germinal center-T cells are the major helpers for GC-B cells and induce class switch recombination. BMC Immunol 2005;6:3.
11. Hjelmstrom P. Lymphoid neogenesis. De novo formation of lymphoid tissue in chronic inflammation through expression of homing chemokines. J Leukoc Biol 2001;69:331–339.
12. Ebert LM, Schaerli P, Moser B. Chemokine-mediated control of T cell traffic in lymphoid and peripheral tissues. Mol Immunol 2005;42:799–809.

13. Aloisi F, Pujol-Borrell R. Lymphoid neogenesis in chronic inflammatory diseases. Nat Rev Immunol 2006;6:205–217.
14. Di Carlo E, D'Antuono T, Contento S, Di Nicola M, Ballone E, Sorrentino C. Quilty effect has the features of lymphoid neogenesis and shares CXCL13-CXCR5 pathway with recurrent acute cardiac rejections. Am J Transpl 2007;7:201–210.
15. McHeyzer-Williams LJ, Malherbe LP, McHeyzer-Williams MG. Checkpoints in memory B-cell evolution. Immunol Rev 2006; 211:255–268.
16. Ye BH, Cattoretti G, Shen Q, Zhang J, Hawe N, de Waard R, Leung C, Nouri-Shirazi M, Orazi A, Chaganti RS, Rothman P, Stall AM, Pandolfi PP, Dalla-Favera R. The BCL-6 proto-oncogene controls germinal-centre formation and Th2-type inflammation. Nat Genet 1997;16:161–170.
17. Pasqualucci L, Migliazza A, Fracchiolla N, William C, Neri A, Baldini L, Chaganti RS, Klein U, Kuppers R, Rajewsky K, Dalla-Favera R. BCL-6 mutations in normal germinal center B cells: Evidence of somatic hypermutation acting outside Ig loci. Proc Natl Acad Sci USA 1998;95:11816–11821.
18. Wolniak KL, Shinall SM, Waldschmidt TJ. The germinal center response. Crit Rev Immunol 2004;24:39–65.
19. Legler DF, Loetscher M, Roos RS, Clark-Lewis I, Baggiolini M, Moser B. B cell-attracting chemokine 1, a human CXC chemokine expressed in lymphoid tissues, selectively attracts B lymphocytes via BLR1/CX CR5. J Exp Med 1998;187:655–660.
20. Moyron-Quiroz JE, Rangel-Moreno J, Kusser K, Hartson L, Sprague F, Goodrich S, Woodland DL, Lund FE, Randall TD. Role of inducible bronchus associated lymphoid tissue (iBALT) in respiratory immunity. Nat Med 2004;10:927–934.
21. Moyron-Quiroz JE, Rangel-Moreno J, Hartson L, Kusser K, Tighe MP, Klonowski KD, Lefrancois L, Cauley LS, Harmsen AG, Lund FE, Randall TD. Persistence and responsiveness of immunologic memory in the absence of secondary lymphoid organs. Immunity 2006;25:643–654.
22. Salmi M, Jalkanen S. Lymphocyte homing to the gut: Attraction, adhesion, and commitment. Immunol Rev 2005;206:100–113.
23. McDermott MR, Bienenstock J. Evidence for a common mucosal immunologic system. I. Migration of B immunoblasts into intestinal, respiratory, and genital tissues. J Immunol 1979;122: 1892–1898.
24. Forrest BD, LaBrooy JT, Robinson P, Dearlove CE, Shearman DJ. Specific immune response in the human respiratory tract following oral immunization with live typhoid vaccine. Infect Immun 1991;59:1206–1209.
25. Zuercher AW, Jiang HQ, Thurnheer MC, Cuff CF, Cebra JJ. Distinct mechanisms for cross-protection of the upper versus lower respiratory tract through intestinal priming. J Immunol 2002;169:3920–3925.
26. Huang Y, Fayad R, Smock A, Ullrich AM, Qiao L. Induction of mucosal and systemic immune responses against human carcinoembryonic antigen by an oral vaccine. Cancer Res 2005;65:6990–6999.
27. Young RH, Srigley JR, Amin MB, Ulbright TM, Cubilla AL. Carcinoma of the prostate gland. In: Rosai J, Sobin LH, editors. Tumors of the prostate gland, seminal vesicles, male urethra, and penis. Washington DC: Armed Forces Institute of Pathology; 2000. 111 p.
28. Steiner GE, Djavan B, Kramer G, Handisurya A, Newman M, Lee C, Marberger M. The picture of the prostatic lymphokine network is becoming increasingly complex. Rev Urol 2002; 4:171–177.
29. Bostwick DG, de la Roza G, Dundore P, Corica FA, Iczkowski KA. Intraepithelial and stromal lymphocytes in the normal human prostate. Prostate 2003;55:187–193.
30. Romagnani S. Regulation of the T cell response. Clin Exp Allergy 2006;36:1357–1366.
31. Bodor J, Fehervari Z, Diamond B, Sakaguchi S. Regulatory T cell-mediated suppression: Potential role of ICER. J Leukoc Biol 2007; 81:161–167.
32. Lim HW, Hillsamer P, Banham AH, Kim CH. Cutting edge: Direct suppression of B cells by CD4+ CD25+ regulatory T cells. J Immunol 2005;175:4180–4183.
33. Lim HW, Hillsamer P, Kim CH. Regulatory T cells can migrate to follicles upon T cell activation and suppress GC-Th cells and GC-Th cell-driven B cell responses. J Clin Invest 2004;114:1640–1649.
34. Chromek M, Slamova Z, Bergman P, Kovacs L, Podracka L, Ehren I, Hokfelt T, Gudmundsson GH, Gallo RL, Agerberth B, Brauner A. The antimicrobial peptide cathelicidin protects the urinary tract against invasive bacterial infection. Nat Med 2006; 12:636–641.
35. Xiao BG, Huang YM, Link H. Tolerogenic dendritic cells: The ins and outs of outcome. J Immunother 2006;29:465–471.
36. Watanabe M, Ueno Y, Yajima T, Iwao Y, Tsuchiya M, Ishikawa H, Aiso S, Hibi T, Ishii H. Interleukin 7 is produced by human intestinal epithelial cells and regulates the proliferation of intestinal mucosal lymphocytes. J Clin Invest 1995;95:2945–2953.
37. Sierro F, Dubois B, Coste A, Kaiserlian D, Kraehenbuhl JP, Sirard JC. Flagellin stimulation of intestinal epithelial cells triggers CCL20-mediated migration of dendritic cells. Proc Natl Acad Sci USA 2001;98:13722–13727.
38. Forster R, Mattis AE, Kremmer E, Wolf E, Brem G, Lipp M. A putative chemokine receptor, BLR1, directs B cell migration to defined lymphoid organs and specific anatomic compartments of the spleen. Cell 1996;87:1037–1047.
39. Ansel KM, Ngo VN, Hyman PL, Luther SA, Forster R, Sedgwick JD, Browning JL, Lipp M, Cyster JG. A chemokine-driven positive feedback loop organizes lymphoid follicles. Nature 2000;406:309–314.
40. Ohl L, Henning G, Krautwald S, Lipp M, Hardtke S, Bernhardt G, Pabst O, Forster R. Cooperating mechanisms of CXCR5 and CCR7 in development and organization of secondary lymphoid organs. J Exp Med 2003;197:1199–1204.
41. Mebius RE. Organogenesis of lymphoid tissues. Nat Rev Immunol 2003;3:292–303.
42. Honda K, Nakano H, Yoshida H, Nishikawa S, Rennert P, Ikuta K, Tamechika M, Yamaguchi K, Fukumoto T, Chiba T, Nishikawa SI. Molecular basis for hematopoietic/mesenchymal interaction during initiation of Peyer's patch organogenesis. J Exp Med 2001;193:621–630.
43. Chen Z, Koralov SB, Kelsoe G. Regulation of humoral immune responses by CD21/CD35. Immunol Rev 2000;176: 194–204.
44. Michie SA, Streeter PR, Bolt PA, Butcher EC, Picker LJ. The human peripheral lymph node vascular addressin. An inducible endothelial antigen involved in lymphocyte homing. Am J Pathol 1993;143:1688–1698.
45. Rosen SD. Ligands for L-selectin: Homing, inflammation, and beyond. Annu Rev Immunol 2004;22:129–156.
46. Stein JV, Rot A, Luo Y, Narasimhaswamy M, Nakano H, Gunn MD, Matsuzawa A, Quackenbush EJ, Dorf ME, von Andrian UH. The CC chemokine thymus-derived chemo-

tactic agent 4 (TCA-4, secondary lymphoid tissue chemokine, 6Ckine, exodus-2) triggers lymphocyte function-associated antigen 1-mediated arrest of rolling T lymphocytes in peripheral lymph node high endothelial venules. J Exp Med 2000;191: 61–76.

47. Carlsen HS, Haraldsen G, Brandtzaeg P, Baekkevold ES. Disparate lymphoid chemokine expression in mice and men: No evidence of CCL21 synthesis by human high endothelial venules. Blood 2005;106:444–446.
48. Miller AM, Lundberg K, Ozenci V, Banham AH, Hellstrom M, Egevad L, Pisa P. CD4+CD25 high T cells are enriched in the tumor and peripheral blood of prostate cancer patients. J Immunol 2006;177:7398–7405.
49. Tschernig T, Pabst R. Bronchus-associated lymphoid tissue (BALT) is not present in the normal adult lung but in different diseases. Pathobiology 2000;68:1–8.
50. Hein WR. Organization of mucosal lymphoid tissue. Curr Top Microbiol Immunol 1999;236:1–15.